New Protonation Microequilibrium Treatment in the Case of Some Amino Acid and Peptide Derivatives Containing a Bis(imidazolyl)methyl Group

Katalin Ösz,* Gábor Lente, and Csilla Kállay

Department of Inorganic and Analytical Chemistry, University of Debrecen, P.O. Box 21, Debrecen H-4010, Hungary

Received: June 9, 2004; In Final Form: August 3, 2004

We present a microequilibrium analysis of a series of amino acid and peptide derivatives containing the chelating bis(imidazol-2-yl)methyl group (BIP, Gly-BIMA, His-BIMA, α-Glu-BIMA, γ-Glu-BIMA, and Phe-His-BIMA). NMR measurements were performed in D_2O to follow the deprotonation steps. The software PSEQUAD and a specialized program written in MATLAB were used to determine the macroscopic and microscopic constants. The method assumes that the effect of pH on the chemical shift of an NMR-active nucleus can be interpreted by adding the independent effects of the protonation of individual sites. For derivatives containing histidine (His-BIMA and Phe-His-BIMA), the deprotonation steps of the second imidazole and the His-imidazole significantly overlap. In the Glu derivatives (α-Glu-BIMA and γ-Glu-BIMA), the amino and the second imidazole p*K* values are separate; the deprotonation processes of the first imidazole nitrogen and the side-chain carboxyl group, however, significantly overlap. In γ-Glu-BIMA, the deprotonation sequence is carboxylate−imidazole(1)−imidazole(2)−amino, while in the case of α-Glu-BIMA, it changes to imidazole(1)−carboxylate−imidazole(2)−amino, according to the microscopic p*k* values. The main advantage of the method is that it does not require the synthesis and NMR microequilibrium analysis of substances modeling the individual parts of the target ligand, in contrast to the methods used by others. The method presented here demands slightly more mathematical and computational power, which is readily available today.

1. Introduction

Peptides containing histidine are the main metal-bonding sites of metalloenzymes. The coordination chemistry of these peptides can be modeled by numerous polyimidazole derivatives, for example, amino acid and peptide derivatives of BIP [bis-(imidazol-2-yl)propionic acid] or BIMA [bis(imidazol-2-yl)-methylamine]. The coordination chemistry of these ligands has been thoroughly investigated.[1−11] However, the acid−base properties of the ligands are also important to explain the coordination behaviors. These multidentate bioligands exist in a great number of protonation forms and inherent fine structures. The physiological role (e.g., enzymatic effect) of these polyfunctional bioligands is structure-dependent. Furthermore, the type and extent of the metal−ligand interactions are also considerably influenced by the protonation fraction of the ligand. Protonations are ubiquitous in every biological medium, so the knowledge of proton-binding characteristics is of great importance for a thorough understanding of effector−receptor and metal−ligand interactions. To specify this for our ligands, it is necessary to determine not only the macroscopic but also the microscopic protonation values (i.e., microspeciation) because the protonation macroconstants calculated for the ligands containing more imidazole groups do not sufficiently characterize the acid−base behavior of the individual proton-binding sites of the ligands as a result of the overlapping deprotonation/protonation steps.[12] The molecules studied in this work are relatively small, so there are no selective indicator groups that could follow the deprotonation of a given protonation site selectively. To deal with this difficulty, we developed a new calculation method for small molecules and overlapping deprotonation steps.

It is well-known that the protonation of a basic site leads to electronic deshielding effects on the adjacent NMR-active nuclei. The magnitude of such effects is dependent on the type of basic center[13] and the distance between the basic center and the NMR-active nucleus. The average chemical shifts of all measurable NMR-active nuclei, as a function of pH (or p*D*), are expected to reflect the fractional protonation of each basic group. Thus, these studies afford a qualitative picture of the protonation sequence. Furthermore, they enable the calculation of parameters characterizing the acid−base properties, as described in the main part of this paper, and also the factors characterizing the effect of a given deprotonation on the chemical shift of any NMR-active nucleus. It is also possible to compare these functions for the ligands with similar structures but eliminate the use of preliminary assumptions.

Earlier literature methods use basically the same idea, but (partly because of the difficulties of the calculations) they could only be used for relatively simple molecules, when there is at least one NMR nucleus whose chemical shift is influenced exclusively by a single protonation site, for each of the overlapping protonation equilibria.[14] In one group of the calculations, "protonation-shift coefficients" are determined and used to calculate the microequilibria of molecules with more complex structures.[15−20] The coefficients seem thoroughly transferable between similar ligands (except for the error of these values, which obviously increases the error of the calculation by increasing the number of the coefficients used); the synthesis of these model (or auxiliary) ligands, however, is often time-consuming and expensive. In addition, however good the model

* To whom correspondence should be sent. E-mail: oszk@delfin.unideb.hu. Tel.: +36-52-512900/2422. Fax: +36-52-489667.

10.1021/jp047515n CCC: $30.25
Published on Web 12/21/2004

ligand is, it is naturally somewhat different from the target ligand, which decreases the transferability of the protonation-shift coefficients. In some cases, finding or preparing suitable model ligands can also be difficult. There is an another way to calculate microscopic constants that uses "interactivity parameters".[21] It has long been recognized that protonation at one site decreases the basicity of other sites in polydentate molecules.[22,23] This effect can be quantified for each pair of groups in terms of interactivity parameters. The interactivity parameters are assumed to be largely invariant in analogous moieties of different compounds and also in various protonation states of the neighboring moiety in the same molecule. This method, however, has the same disadvantages as the one using protonation-shift coefficients.

In another sequence of thought, "group constants" are defined instead of microscopic constants.[24] Group constants can be deduced from microconstants through simplifications. These simplifications have definite chemical preconditions, which makes the use of this method limited as well. The most usual (for rigid molecules, the only) reason for having microconstants of the same group that differ from one another is the electron-withdrawing effect, which occurs when the adjacent groups are protonated. This causes a larger or smaller decrease in the basicity of the group in question. The effect is significant if the adjacent group is separated by a sufficiently low number of intervening atoms from the given group; that is, the static inductive effect reaches the group under consideration. Among microconstants belonging to the same group, the largest p*k* value refers to the proton association when no other sites are protonated and the smallest one refers to the fully protonated ligand. The limitation of the method is that if the difference between two extreme microscopic constants is too small (i.e., it does not exceed the error of the microconstant determination), then all of the microconstants of the same group are virtually equal. Accordingly, all of them can be quantified in one parameter called a group constant. In these systems, the number of unknown group constants is equal to the number of macroconstants; that is, the group constants can be calculated from the macroscopic constants measured in traditional ways.

2. Experimental Section

2.1. Materials. Detailed accounts of the synthesis, purification, and characterization of bis(imidazol-2-yl) derivatives, namely, BIP,[25] Gly-BIMA,[10] α-Glu-BIMA, γ-Glu-BIMA,[11] His-BIMA,[5] and Phe-His-BIMA,[3] were given in earlier publications.

2.2. Potentiometric Titrations. The pH-metric titrations in the pH range 2.2−11.0 were performed in 4 cm^3 vessels at a ligand concentration of 4×10^{-3} mol/dm^3. Argon was bubbled through the samples to ensure the absence of oxygen and to stir the solutions. All pH-metric measurements were carried out at 298 K and at a constant ionic strength of 0.2 mol/dm^3 KCl. The measurements were carried out with a Radiometer pHM 84 pH-meter equipped with a 6.0234.100 combination glass electrode (Metrohm) and a Dosimat 715 automatic buret (Metrohm) containing carbonate-free potassium hydroxide in a known concentration. The pH readings were converted to hydrogen ion concentrations using the method described by Irving et al.[26]

2.3. NMR−pH Titrations. A pH-dependent series of ^{1}H NMR spectra were recorded on a Bruker 360 MHz instrument at 25 °C. D_2O was used as a solvent. The pH measurements in the pH range 1.5−12.2 were performed in 2 cm^3 vessels, not in the NMR tubes, at a ligand concentration of 0.01 mol/dm^3. Different concentrations (1, 0.1, and 0.01 mol/dm^3) of NaOD and DCl solutions in D_2O were used to adjust the pH. The pH readings were converted into p*D* values using eq 4. Chemical shifts were referenced to sodium 3-(trimethylsilyl)-1-propanesulfonate.

2.4. Data Analysis. To fit our model equations to the experimental NMR−pH profiles, the macroscopic p*K* values and the NMR spectra of the deprotonated, singly protonated, doubly protonated (etc.), and fully protonated individual macroscopic species were determined using a general computational program, PSEQUAD,[27] which uses eq 1:

$$n\mathrm{H}^+ + \mathrm{L} = \mathrm{H}_n\mathrm{L} \qquad \beta_{\mathrm{H}_n\mathrm{L}} = \frac{[\mathrm{H}_n\mathrm{L}]}{[\mathrm{H}]^n[\mathrm{L}]} \tag{1}$$

This is the same computational program that was used earlier to calculate the macroscopic protonation constant values on the basis of the pH-potentiometric titrations at 25 °C and at a constant ionic strength of 0.2 mol/dm^3 KCl.

3. Results and Discussion

3.1. NMR Titrations. In the case of Phe-His-BIMA (the only ligand containing two chirality centers), the presence of two isomers was indicated by the duplication of all ^{1}H NMR signals. The ratio of the two isomers was about 2:1. After the NMR sample (in D_2O and at pH = 3.11) was heated to 340 K, the ratio of the two isomers did not change and there was no specific NMR line broadening, indicating the absence of hindered rotamers. Two-dimensional correlation spectroscopy and nuclear Overhauser enhancement spectroscopy measurements combined with water suppression also confirmed the absence of rotatory isomers and proved the presence of two diastereoisomers with LL and DL configurations on the Phe and His moieties. This could be a consequence of some racemization occurring during the synthesis of these ligands.

During the microconstant calculations, we used the NMR signals for the LL diastereoisomer. The easily measurable NMR signals for the DL diastereoisomer show the same tendency as that observed for the LL diastereoisomer. Some of the NMR signals for the DL diastereoisomer, however, overlapped with more-intense NMR signals of the LL diastereoisomer, so we could not carry out the microequilibrium analysis of the DL diastereoisomer. Upon heating of the sample to 340 K, the total deuteration of the CH groups of both diastereoisomers was also observed.

In addition, it is known from the literature that a slight degree of N(1)H−N(3)H isomerization (or N^τH−N^πH tautomerization) occurs in His derivatives. However, both literature data[28] and our measurements show that there is practically no N(3)H isomer in the solutions of our His-containing ligands (His-BIMA and Phe-His-BIMA). When the bis(imidazol-2-yl)methyl groups are investigated, the positions of the N(1)H and N(3)H groups are the same, so the question of N(1)H−N(3)H isomerization does not even arise. Accurate pH measurements in H_2O are readily performed using glass electrodes and appropriate calibration procedures, such as the use of standard buffers. The same is possible for the corresponding p*D* measurements in D_2O using the required buffers. In laboratory practice, however, a related quantity called pH* is used, which is a direct reading in a D_2O solution of the "H_2O-calibrated" pH meter. The pH* values can be converted to p*D* values using the relationship between H^+ and D^+ ions, according to the Gross−Butler−Purlee theory (eq 2).[29−31] This is based on literature measurements of acids or bases dissolved at the same concentrations in H_2O and D_2O.

$$pD = pH^* + 0.44 \quad (2)$$

Moreover, the binding affinities of protonating groups are, in general, different for H^+ and D^+ and also for solvents of different ionic strengths. In the case of pH-metric measurements, the use of a high ionic strength is standard; in the case of NMR measurements, however, the addition of salts is preferably avoided because high ionic strengths often lead to deterioration of the spectra. The effect of ionic strength has to be taken into consideration. By expanding the theory of Krezel and Bal[32] to $I = 0.2$ mol/dm^3, we could find a relationship between pH and pD on the basis of the pK_w values in H_2O and D_2O (eq 3):

$$pD = 1.084pH \quad (3)$$

Combining eqs 2 and 3 gives

$$pH = 0.930pH^* + 0.40 \quad (4)$$

3.2. Computational Details. Stepwise protonation constants for the ligands in Scheme 1, calculated from potentiometric ($T = 25$ °C and $I = 0.2$ mol/dm^3 KCl) and ^{1}H NMR ($T = 25$ °C and $I \rightarrow 0$) titrations, are summarized in Table 1. The general computational program PSEQUAD was used to calculate the pK values from both the pH-potentiometric and the NMR titrations. The NMR splitting scheme carries no information about the protonation steps, so only the chemical shifts were used in the calculations, without taking the coupling constants into account.

Equation 4 was used to correct the ^{1}H NMR data to the conditions of the pH-potentiometric measurements (last section of Table 1). The data in Table 1 show that the pK values measured at an ionic strength of 0.2 mol/dm^3 (by pH-metric titrations), those calculated for an ionic strength of 0.2 mol/dm^3, and those for H_2O solvent from NMR titrations are in good agreement.

By using the computational program PSEQUAD, not only could the macroscopic pK values be calculated on the basis of the NMR titrations, but the individual NMR spectra of the ligands containing one, two, three, and so forth protons (L, HL, H_2L, ..., H_nL) could also be resolved. In the second step, all NMR signals were normalized, that is, transformed to values between 0 and 1. In this way, 0 corresponds to the chemical shift of a given NMR-active site in the deprotonated ligand (L) and 1 corresponds to the fully protonated ligand (H_3L for L = BIP and Gly-BIMA and H_4L for L = His-BIMA, Phe-His-BIMA, α-Glu-BIMA, and γ-Glu-BIMA; see Table 2 for the distribution of protons among the protonation sites).

After the PSEQUAD calculations are performed, the normalized data matrix **D** is obtained. In the rest of the text, the ligand Phe-His-BIMA will be used as an example to illustrate how the method is used. The normalized data matrix for Phe-His-BIMA is

$$\mathbf{D} = \begin{pmatrix} 0.1013 & 0.0414 & 0.0920 & 0.0503 & 0.7879 \\ 0.6181 & 0.0923 & 0.6847 & 0.0982 & 0.9464 \\ 0.8965 & 0.3564 & 0.8650 & 0.3744 & 0.9500 \\ 1.0000 & 1.0000 & 1.0000 & 1.0000 & 1.0000 \end{pmatrix}$$

In this matrix, row q contains the normalized chemical shifts of the species H_qL ($q = 1-4$). Because the chemical shifts of H_4L are used in the normalization, all of the values in row 4 are equal to 1. Still, they have to be included in the matrix and subsequent calculations for reasons that will be explained later. (Figure 1 shows the normalized chemical shifts of individual macrospecies for Phe-His-BIMA.)

The calculation method introduced in this paper uses the assumption that the change in the chemical shift of a specific NMR-active nucleus can be calculated by the linear combination of the separate and independent effects of the protonation of individual sites.[33,34] We designated the protonation sites of the ligands with capital letters (X, Y, W, and Z) and the NMR-active nuclei with numbers (1, 2, 3, etc.). When two equivalent sites were present, we used X to refer to the first protonation of the two equivalent sites independently of where this protonation occurs and Y referred to the second protonation in a similar manner. This method was used for Phe-His-BIMA, for example. Only ^{1}H NMR was used, and it should be noted that not all of the nonlabile ^{1}H nuclei of the ligand are useful because some of them may overlap with the solvent signal in part of the pH range studied. Scheme 1 shows how the protonation sites and useful NMR-active nuclei are distributed in Phe-His-BIMA. For each protonation site/NMR-active nucleus pair, a factor (C) characteristic of their interaction can be defined; for example, the effect of the deprotonation of "site Y" on the NMR signal of "nucleus 3" is given as C_{Y3}. In a microscopic system containing n protonation sites and m useful NMR-active nuclei, the total number of factors is $m \times n$. These factors can be arranged as elements of a matrix **C**, which is a 5×4 matrix for Phe-His-BIMA because chemical shifts for five useful nuclei could be followed over the entire pH range.

$$\mathbf{C} = \begin{pmatrix} C_{X1} & C_{X2} & C_{X3} & C_{X4} & C_{X5} \\ C_{Y1} & C_{Y2} & C_{Y3} & C_{Y4} & C_{Y5} \\ C_{W1} & C_{W2} & C_{W3} & C_{W4} & C_{W5} \\ C_{Z1} & C_{Z2} & C_{Z3} & C_{Z4} & C_{Z5} \end{pmatrix}$$

It is clear that every factor is between 0 and 1 because of the normalization already discussed.

In our experience, it is much more advantageous to use conditional probabilities in the calculations rather than microequilibrium constants for two fundamental reasons. First, the normalized chemical shifts of the individual microforms can be calculated in a very simple way when conditional probabilities are used instead of microequilibrium constants. Second, in any given system, the number of possible microequilibrium constants exceeds the number of conditional probabilities and the microequilibrium constants in general are not independent, which results in considerable complications. These problems are avoided when conditional probabilities are used: all conditional probabilities are between 0 and 1, and the sum of the conditional probabilities for all of the different forms of one macrospecies is 1. In this work, the subscripted letters a (for different microforms of H_3L), b (H_2L), and c (HL) are used to refer to conditional probabilities. Schemes 1 and 2 show the designation of all possible microforms of Phe-His-BIMA. This example also indicates that the symmetry of the ligand can also be taken into account. There are two equivalent protonation sites in Phe-His-BIMA; thus, the number of microforms for HL is only three. Similar considerations apply for H_2L (four different forms) and H_3L (three different forms).

The following equations hold for the conditional probabilities:

$$a_1 + a_2 + a_3 = 1$$

$$b_1 + b_2 + b_3 + b_4 = 1$$

$$c_1 + c_2 + c_3 = 1$$

Because of these equations, a_3, b_4, and c_3 were not used as parameters in the final calculations. Their values were computed

SCHEME 1

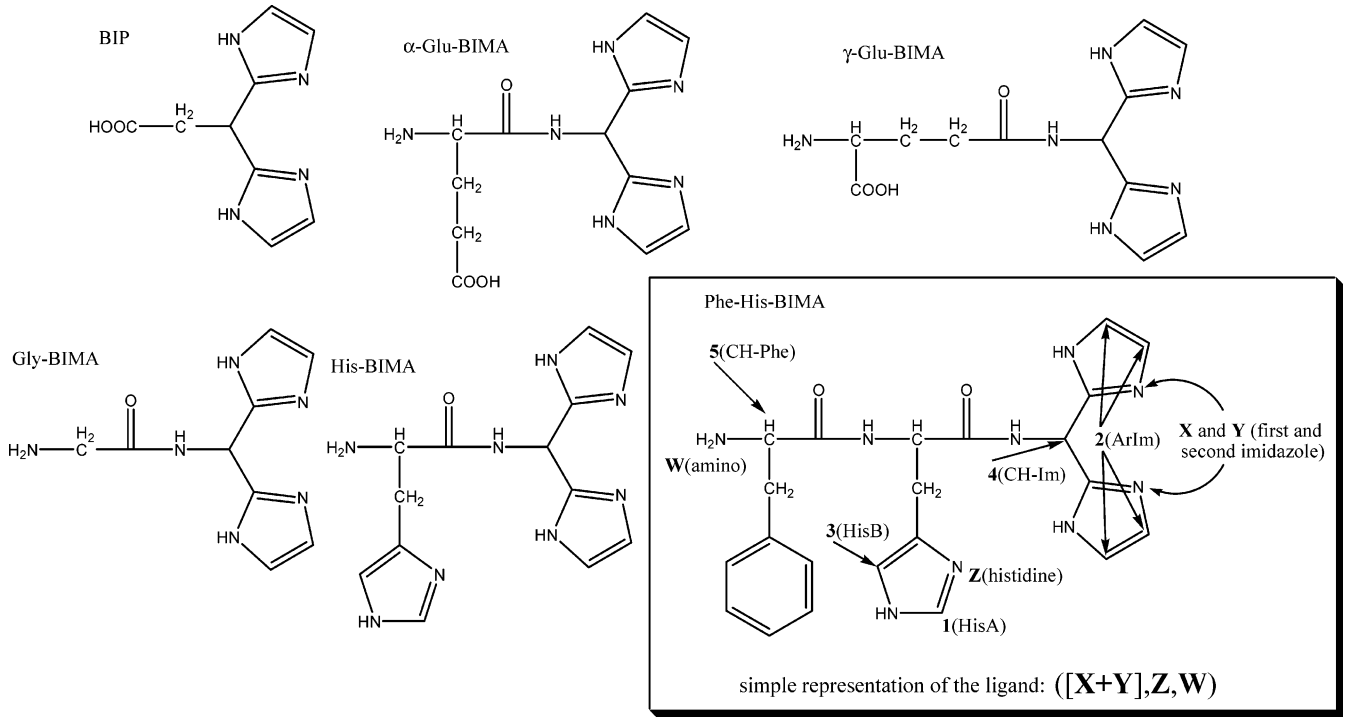

TABLE 1: Protonation Constants and p*K* Values of the Ligands Calculated from pH-Potentiometric (T = 25 °C, I = 0.2 mol/dm³ KCl) and ^{1}H NMR Titrations (T = 25 °C, No Ionic Strength)

	BIP	Gly-BIMA	α-Glu-BIMA	γ-Glu-BIMA	His-BIMA	Phe-His-BIMA	conditions
$\log \beta_{H_4L}$			19.48	20.08	20.23	21.48	*a*
$\log \beta_{H_3L}$	14.31	16.68	16.79	18.29	17.62	18.65	*a*
$\log \beta_{H_2L}$	11.52	13.46	13.05	14.88	13.09	13.58	*a*
$\log \beta_{HL}$	6.90	7.95	7.53	9.05	7.28	7.27	*a*
p*K*(imidazole(1))	**4.62**	**3.22**	**2.69**	**3.41**	**2.61**	**2.83**	*a*
p*K*(imidazole(2))	**6.90**	**5.51**	**5.52**	**5.83**	**4.53**	**5.07**	*a*
p*k*(histidine)					**5.81**	**6.31**	*a*
p*K*(amino)		**7.95**	**7.53**	**9.05**	**7.28**	**7.27**	*a*
p*K*(carboxylic)	**2.79**		**3.74**	**1.79**			*a*
pK_1	2.57(9)	3.03(9)	2.1(1)	1.3(2)	2.38(9)	2.83(7)	*b*
pK_2	4.53(9)	5.48(6)	3.76(9)	3.42(6)	4.22(9)	5.46(2)	*b*
pK_3	6.97(8)	8.09(3)	5.62(6)	5.85(2)	5.50(7)	6.33(5)	*b*
pK_4			7.77(2)	9.19(3)	7.44(4)	7.15(2)	*b*
pK_1	**2.80**	**3.23**	**2.40**	**1.62**	**2.62**	**3.04**	*c*
pK_2	**4.62**	**5.51**	**3.90**	**3.59**	**4.33**	**5.08**	*c*
pK_3	**6.89**	**7.93**	**5.63**	**5.85**	**5.52**	**6.29**	*c*
pK_4			**7.63**	**8.95**	**7.32**	**7.06**	*c*

[a] Potentiometric measurements (T = 25 °C, I = 0.2 mol/dm³ KCl). Data from references: BIP, Gly-BIMA,[6] His-BIMA, Phe-His-BIMA,[3] α- and γ-Glu-BIMA.[11] [b] ^{1}H NMR titrations (T = 25 °C, no ionic strength, D_2O). [c] ^{1}H NMR data corrected to I = 0.2 mol/dm³ and H_2O as a solvent.

from the other conditional probabilities. Therefore, the number of independent conditional probabilities to be determined is seven.

In the next step, the proton fraction matrix (**Q**) is introduced. The elements of row q in this matrix show what fraction of an individual group is protonated in the average macrospecies H_qL. Consequently, **Q** is always a square matrix with $n \times n$ elements. The conditional probabilities define all of the elements of this matrix unambiguously. For Phe-His-BIMA and all ligands with four protonation sites and the same symmetry, **Q** is given as

$$\mathbf{Q} = \begin{pmatrix} c_1 & 0 & c_2 & c_3 \\ b_1 + b_2 + b_3 & b_1 & b_2 + b_4 & b_3 + b_4 \\ 1 & a_2 + a_3 & a_1 + a_2 & a_1 + a_3 \\ 1 & 1 & 1 & 1 \end{pmatrix}$$

It should be pointed out that X and Y do not refer to specific protonation sites in the notation we used. Rather, site X is considered to be occupied if at least one of the two equivalent bis(imidazolyl) sites is protonated, hence the trivial value of 1 for Q_{31} (in all microforms of H_3L, at least one of the two equivalent sites must be protonated). Similarly, site Y is considered to be occupied if both of the two equivalent bis-(imidazolyl) sites are protonated, hence the trivial value of 0 for Q_{12} (no microform of HL can feature both equivalent sites protonated). The number of elements in the proton fraction matrix is usually different from the number of conditional probabilities. However, some elements in the matrix are trivial. In the example shown, the number of nontrivial elements (i.e., elements different from 0 or 1) equals the number of conditional probabilities.

The final matrix equation giving the normalized chemical shifts is

$$\mathbf{QC} = \mathbf{D} \qquad (5)$$

TABLE 2: Distribution of the Protons in the Case of Singly, Doubly, and So Forth Protonated Species (HL, H_2L, etc.) among the Protonation Sites[a]

ligand (L)	protonation site	HL	H_2L	H_3L
BIP	imidazole(1)	0.999	1.0000	
	imidazole(2)	0.000	0.9433	
	carboxylic	0.001	0.0567	
Gly-BIMA	imidazole(1)	0.0900	1.0000	
	imidazole(2)	0.0000	0.0000	
	amino	0.9100	1.0000	
α-Glu-BIMA	imidazole(1)	0.0000	0.7971	1.0000
	imidazole(2)	0.0000	0.0099	0.1464
	carboxylic	0.1115	0.2114	0.8720
	amino	0.8885	0.9817	0.9817
γ-Glu-BIMA	imidazole(1)	0.0194	0.9759	1.0000
	imidazole(2)	0.0000	0.0101	0.9537
	carboxylic	0.0260	0.0260	0.0584
	amino	0.9546	0.9879	0.9879
His-BIMA	imidazole(1)	0.0600	0.4785	1.0000
	imidazole(2)	0.0000	0.0203	0.1588
	histidine	0.0050	0.5661	0.8412
	amino	0.9350	0.9350	1.0000
Phe-His-BIMA	imidazole(1)	0.1362	0.3135	1.0000
	imidazole(2)	0.0000	0.0000	0.0682
	histidine	0.0000	0.6962	0.9416
	amino	0.8638	0.9902	0.9902

[a] For L, the number of protons is 0, and for H_3L (L = BIP or Gly-BIMA) and H_4L (L = α-Glu-BIMA, γ-Glu-BIMA, His-BIMA, or Phe-His-BIMA), the number of protons is 1 for all protonation sites.

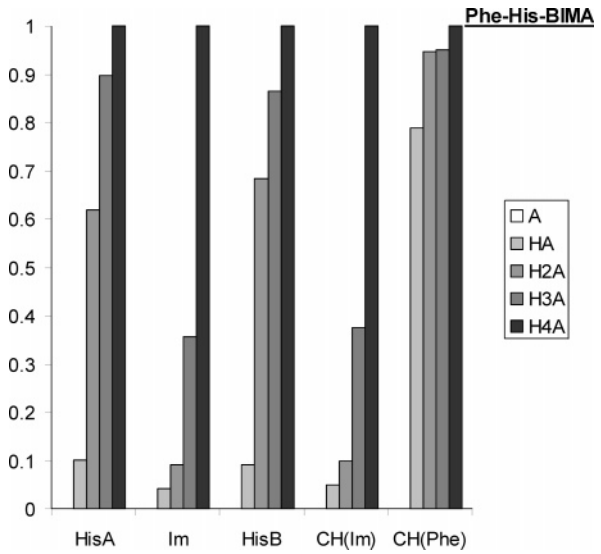

Figure 1. Normalized chemical shifts of individual macrospecies for Phe-His-BIMA at all macroscopic protonation stages.

To solve the problem, one has to find the values for each factor and conditional probability that give the best fit to the experimental data. Using the least-squares method for this problem, the residual matrix **res** can be calculated as

$$\mathbf{res} = \mathbf{D} - \mathbf{QC}$$

Summing the squares of all elements in matrix **res** gives the sum of residuals, and the best fit is where the sum of residuals is minimal.

At this point, the reason for including row 4 in data matrix **D** can also be explained. The method presented in this work is based on the changes in chemical shifts as a function of pH. Changes are measured relative to the chemical shifts of the fully deprotonated ligand, which are set to 0 during normalization. Thus, no experimental data corresponding to the totally deprotonated ligand L can be informative. For the remaining four macroforms, differences of chemical shifts are measured with some experimental error. This is true for H_4L as well, irrespective of the fact that its signals are used to provide the unit for normalization. Although the values in row 4 of data matrix **D** are set to 1 by normalization, there is no reason to handle these points differently from the rest of the data set. In other words, the elements of row 4 in matrix **QC** do not have to be exactly 1 because these data have some experimental error as well and should be part of the least-squares minimalization procedure.

SCHEME 2

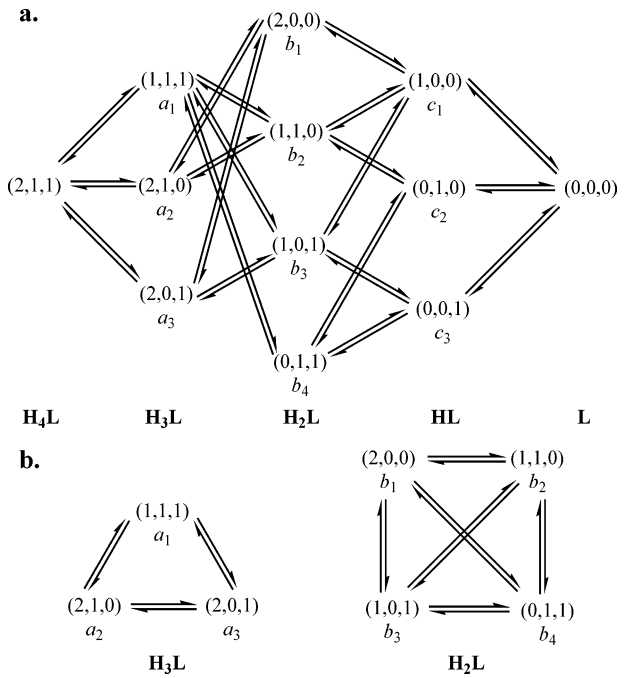

Turning back to the minimum-finding problem, it can be seen that the number of parameters to be determined is 27 (20 *C* factors and 7 independent conditional probabilities), whereas the number of data points available is 20. There are more parameters than data points, which may suggest, at first sight, that there are an infinite number of parameter sets that exactly satisfy eq 5 and, therefore, the parameters cannot be determined. However, this statement is only correct mathematically if the parameters can assume any real values. In fact, the physically meaningful parameter space is very seriously limited in a variety of ways.

First of all, all of the *C* factors and the conditional probabilities should be between 0 and 1. In addition, a number of somewhat system-specific, trivial chemical considerations further limiting the meaningful combinations of conditional probabilities and *C* factors can be taken into account in every case. One such observation is that a protonation site cannot lose protons when the concentration of free H^+ increases. This means that any element in matrix **Q** cannot be smaller than the one right above it.

$$c_1 \le b_1 + b_2 + b_3$$

$$b_1 \le a_2 + a_3$$

$$c_2 \le b_2 + b_4 \le a_1 + a_2$$

$$c_3 \le b_3 + b_4 \le a_2 + a_3$$

It should be noted that exceptions to this rule are known. Anomalous protonation sequences are usually a consequence of structural factors such as electrostatic repulsion of adjacent

sites.[35] In certain cases, one or more of the constraints introduced in the previous equations may have to be left out. One possible indication of such an anomalous protonation sequence can be an extremum on one of the experimentally measured chemical shift versus pH curves. However, for the ligands studied in this work, there was no reason to suspect that anomalous protonation sequences had to be considered.

Another observation is that the chemical shift of an NMR-active nucleus is influenced more by the protonation of nearby sites than that of sites farther away. In a few cases, the NMR-active nucleus and the group are so far away from each other that the interaction between them can be neglected, meaning that a few elements of matrix **C** cannot be different from 0. Specifically for Phe-His-BIMA, the following constraints were used:

$$C_{X5} = 0, \quad C_{Y5} = 0, \quad C_{Z2} = 0, \quad C_{Z4} = 0, \quad C_{X1} \le C_{Z1},$$
$$C_{Y1} \le C_{Z1}, \quad C_{W1} \le C_{Z1}, \quad C_{W2} \le C_{X2}, \quad C_{W2} \le C_{Y2},$$
$$C_{X3} \le C_{Z3}, \quad C_{Y3} \le C_{Z3}, \quad C_{W3} \le C_{Z3}, \quad C_{W4} \le C_{X4},$$
$$C_{W4} \le C_{Y4}, \quad C_{Z5} \le C_{W5}$$

The best fit was searched for by minimizing the sum of the squared residuals in the parameter space defined by the constraints. Specialized software using the simplex method was written in the programming language MATLAB for this purpose. This algorithm did not use weighing because the nucleus-dependent differences between the chemical shifts of the fully protonated and deprotonated ligands (used in normalization) were well within a factor of 2 for all ligands. This means that the sensitivities of the individual nuclei were quite similar. If the sensitivities are significantly different or the chemical shifts of heteronuclei are used simultaneously in a problem, an appropriate weighing method should be used. Guidelines for using weights are given in the Supporting Information.

The final results for the example ligand Phe-His-BIMA are as follows:

$$a_1 = 0.93(1), \quad a_2 = 0.01(1), \quad a_3 = 0.06(1)$$

$$b_1 = 0, \quad b_2 = 0.010(1), \quad b_3 = 0.304(1), \quad b_4 = 0.687(1)$$

$$c_1 = 0.136(6), \quad c_2 = 0, \quad c_3 = 0.86(1)$$

$$\mathbf{Q} = \begin{pmatrix} 0.1362 & 0 & 0 & 0.8638 \\ 0.3135 & 0 & 0.6962 & 0.9902 \\ 1 & 0.0682 & 0.9416 & 0.9902 \\ 1 & 1 & 1 & 1 \end{pmatrix}$$

$$\mathbf{C} = \begin{pmatrix} 0.0938 & 0.3077 & 0 & 0.3278 & 0 \\ 0.0938 & 0.6924 & 0.0813 & 0.6722 & 0 \\ 0.7224 & 0 & 0.8070 & 0 & 0.0712 \\ 0.0989 & 0 & 0.1110 & 0 & 0.9096 \end{pmatrix}$$

$$\mathbf{res} = \begin{pmatrix} -0.0031 & 0.0005 & 0.0038 & -0.0057 & -0.0022 \\ 0.0122 & 0.0041 & -0.0129 & 0.0046 & 0.0038 \\ -0.0183 & -0.0014 & 0.0103 & -0.0007 & 0.0177 \\ 0.0087 & 0.0001 & -0.0007 & 0.0000 & -0.0193 \end{pmatrix}$$

Rigorous mathematical analysis published by Szakács and Noszál showed that full microequilibrium analysis is theoretically impossible for a ligand with a pair of equivalent and two more different protonation sites.[36] However, the authors also noted that this fact only precludes full microequilibrium analysis (meaning the determination of every single microequilibrium constant, no matter how minor the species involved are) without additional a priori assumptions. In this work, we carry out only a partial analysis because the conditional probabilities of minor species remain undetermined. In addition, we also introduce a priori assumptions by setting a few *C* factors to 0 and assuming inequities between *C* factors and conditional probabilities. It should also be added that a rigorous experimental equilibrium evaluation of very minor species does not seem to be particularly feasible, in general, because those very minor species are unlikely to contribute to any kind of experimentally detected signal.

3.3. Comparison of Macroscopic and Microscopic Constants of the Ligands. The main advantage of separating the calculation of the macroscopic p*K* values and normalized spectra of the macrospecies from the calculation of the factors and conditional probabilities of the microspecies is that we can also separate the errors of these two kinds of values. Measuring more spectra can make the macroscopic p*K* values and the values of the normalized spectra of the macrospecies more exact (and this is necessary when the error of these data is high) but has no effect on the error of the microspecies calculations.

Even after the PSEQUAD calculations were performed without any microconstant calculations, the main tendencies of the protonation processes can be seen from the figures showing the normalized NMR signals for all of the NMR-active nuclei and all of the macrospecies: a substantial change of a given normalized NMR signal indicates a high probability of deprotonation/protonation of a group close to the NMR-active nucleus. On the basis of this observation, we can conclude that, in the case of Gly-BIMA, the first and second p*K* values belong to the two imidazoles [CH(Im) and aromatic imidazole normalized spectra change in the first and second deprotonation steps but not in the third one] and the amino p*K* is the highest one [CH_2 normalized spectra indicating mainly the protonation stage of the amino group are almost the same as those for H_3L, H_2L, and HL (1.00, 0.93, and 0.83, repectively) and are very different for those of L (0.00)]. In the BIP ligand, however, the deprotonation of the carboxyl group precedes the deprotonation of the imidazoles. For derivatives containing histidine (His-BIMA and Phe-His-BIMA), the deprotonation steps of the second imidazole and those of the His-imidazole significantly overlap; the highest and the lowest p*K* values, however, belong to the amino and the first imidazole groups, respectively. Among the NMR signals of His-BIMA, CH(His) is the best indicator of the amino group, and the normalized spectrum for this group changes as follows: 1.00 (H_4L), 0.88 (H_3L), 0.80 (H_2L), 0.59 (HL), and 0.00 (L). The imidazole groups are indicated, for example, by the CH(Im) signals, which are 1.00, 0.53, 0.39, 0.08, and 0.00 for H_4L, H_3L, H_2L, HL, and L, respectively. The values for Phe-His-BIMA are 1.00, 0.95, 0.94, 0.79, and 0.00 for the CH(Phe) group close to the amino protonation site and 1.00, 0.37, 0.10, 0.05, and 0.00 for the CH(Im) signals. In the Glu derivatives (α-Glu-BIMA and γ-Glu-BIMA), the amino p*K* values are separate; the imidazole p*K* values and the side-chain carboxyl p*K* values overlap. In γ-Glu-BIMA, the deprotonation starts at the carboxylate group, while in the case of α-Glu-BIMA, it starts at the first imidazole. The main advantage of using normalized (or even the calculated) NMR spectra for the ligand forms containing integer protons is that difficult mathematical calculation methods are not needed to get information about the deprotonation/protonation sequence of a compound.

TABLE 3: Microscopic Deprotonation Constants for Given Microspecies[a] and Microscopic Protonation Constants for 50% Degree of Protonation (p$k^{1/2}$)[b]

	BIP	Gly-BIMA	α-Glu-BIMA	γ-Glu-BIMA	His-BIMA	Phe-His-BIMA
p*k*(imidazole(1))	$^{(2,0)\rightarrow(1,0)}$4.60(1)	$^{(2,1)\rightarrow(1,1)}$3.22(1)	$^{(2,1,1)\rightarrow(1,1,1)}$2.76(2) $^{(2,0,1)\rightarrow(1,0,1)}$2.96(7)	$^{(2,1,1)\rightarrow(1,1,1)}$3.13(9) $^{(2,0,1)\rightarrow(1,0,1)}$3.40(1)	$^{(2,1,1)\rightarrow(1,1,1)}$2.69(5) $^{(2,0,1)\rightarrow(1,0,1)}$4.1(2) $^{(2,0,0)\rightarrow(1,0,0)}$5.3(6)	$^{(2,1,1)\rightarrow(1,1,1)}$2.86(1) $^{(2,0,1)\rightarrow(1,0,1)}$4.35(9)
p*k*(imidazole(2))	$^{(1,0)\rightarrow(0,0)}$6.90(1)	$^{(1,1)\rightarrow(0,1)}$5.55(1) $^{(1,0)\rightarrow(0,0)}$9.00(5)	$^{(1,1,1)\rightarrow(0,1,1)}$4.36(4) $^{(1,1,0)\rightarrow(0,1,0)}$4.4(4) $^{(1,0,1)\rightarrow(0,0,1)}$5.46(2)	$^{(1,1,1)\rightarrow(0,1,1)}$3.9(5) $^{(1,0,1)\rightarrow(0,0,1)}$5.84(1) $^{(1,0,0)\rightarrow(0,0,0)}$7.3(3)	$^{(1,1,1)\rightarrow(0,1,1)}$4.74(6) $^{(1,0,1)\rightarrow(0,0,1)}$5.46(3) $^{(1,0,0)\rightarrow(0,0,0)}$6.1(3)	$^{(1,1,1)\rightarrow(0,1,1)}$5.20(1) $^{(1,0,1)\rightarrow(0,0,1)}$5.86(2) $^{(1,0,0)\rightarrow(0,0,0)}$6.40(3)
p*k*(histidine)					$^{(2,1,1)\rightarrow(2,0,1)}$3.4(1) $^{(1,1,1)\rightarrow(1,0,1)}$4.84(6) $^{(0,1,1)\rightarrow(0,0,1)}$5.56(3) $^{(1,1,0)\rightarrow(1,0,0)}$5.7(4)	$^{(2,1,1)\rightarrow(2,0,1)}$4.06(7) $^{(1,1,1)\rightarrow(1,0,1)}$5.56(2) $^{(0,1,1)\rightarrow(0,0,1)}$6.21(1) $^{(1,1,0)\rightarrow(1,0,0)}$5.2(4)
p*k*(amino)		$^{(1,1)\rightarrow(1,0)}$6.56(5)	$^{(2,1,1)\rightarrow(2,1,0)}$4.4(3) $^{(2,0,1)\rightarrow(2,0,0)}$4.9(4) $^{(1,1,1)\rightarrow(1,1,0)}$5.7(3) $^{(0,1,1)\rightarrow(0,1,0)}$5.8(1) $^{(0,0,1)\rightarrow(0,0,0)}$7.48(2)	$^{(1,0,1)\rightarrow(1,0,0)}$7.5(3) $^{(0,1,1)\rightarrow(0,1,0)}$5.8(8) $^{(0,0,1)\rightarrow(0,0,0)}$9.04(1)	$^{(2,0,1)\rightarrow(2,0,0)}$5.4(4) $^{(1,1,1)\rightarrow(1,1,0)}$5.8(1) $^{(1,0,1)\rightarrow(1,0,0)}$6.6(3) $^{(0,0,1)\rightarrow(0,0,0)}$7.25(2)	$^{(2,1,1)\rightarrow(2,1,0)}$4.8(4) $^{(1,1,1)\rightarrow(1,1,0)}$7.0(4) $^{(1,0,1)\rightarrow(1,0,0)}$6.66(5) $^{(0,0,1)\rightarrow(0,0,0)}$7.21(1)
p*k*(carboxylic)	$^{(2,1)\rightarrow(2,0)}$2.82(1) $^{(1,1)\rightarrow(1,0)}$3.37(9)		$^{(2,1,1)\rightarrow(2,0,1)}$3.58(7) $^{(1,1,1)\rightarrow(1,0,1)}$3.78(2) $^{(0,1,1)\rightarrow(0,0,1)}$4.88(4) $^{(0,1,0)\rightarrow(0,0,0)}$6.5(1)	$^{(2,1,1)\rightarrow(2,0,1)}$1.81(1) $^{(1,1,1)\rightarrow(1,0,1)}$2.08(9) $^{(0,1,1)\rightarrow(0,0,1)}$4.0(6) $^{(0,1,0)\rightarrow(0,0,0)}$7.2(5)		
p$k^{1/2}$(imidazole(1))	4.4	3.2	2.8	3.4	2.8	2.9
p$k^{1/2}$(imidazole(2))	6.9	5.6	5.3	5.8	5.2	5.4
p$k^{1/2}$(histidine)					5.3	6.0
p$k^{1/2}$(amino)		7.8	7.4	9.0	7.2	7.2
p$k^{1/2}$(carboxylic)	2.8		3.9	1.8		

[a] The sequence of numbering is imidazoles−carboxylic−histidine−amino. [b] Standard deviations of the last digits are in parentheses.

When the conditional probabilities for the microspecies (a_1, a_2, a_3, b_1, b_2, b_3, b_4, c_1, c_2, and c_3) and the macroscopic p*K* values are used, the isomerization and protonation microconstants (p*k*) for an arbitrary microequilibrium in Schemes 2a,b can be calculated using the following equations:

$$\mathrm{p}k^{(2,0,1)\rightarrow(1,1,1)}_{\text{isomerisation}} = -\log\left(\frac{[(2,0,1)]}{[(1,1,1)]}\right) = -\log\left(\frac{a_3}{a_1}\right) \qquad (6)$$

$$\mathrm{p}k^{(2,1,0)\rightarrow(2,0,0)}_{\text{protonation}} = -\log\left(\frac{[(2,0,0)][\mathrm{H}^+]}{[(2,1,0)]}\right) = -\log\left(\frac{[\mathrm{H_2L}]b_1[\mathrm{H}^+]}{[\mathrm{H_3L}]a_2}\right) = \mathrm{p}K_3 - \log\left(\frac{b_1}{a_2}\right) \qquad (7)$$

Some of these data are collected in Table 3.

From these data, the general tendency is that, as the number of protons on a particular ligand decreases, the p*k* values for a particular protonation site increase, in agreement with the expectation[22] that the fewer protons (i.e., the less positive charge) a ligand has, the more difficult it is to remove another proton. In some cases, when the standard deviation of the conditional probabilities is too high relative to its value (it happens mainly when at least one of the conditional probability values included in eq 7 is too low), the error of the microscopic constants determined can be relatively high, as we can see from the data of Table 3. These values cannot be determined better by more exact NMR measurements: the error is caused by the low conditional probabilities and not by the inaccuracy of the measurement. On the other hand, because of the low conditional probabilities, these values have little importance.

The third and most useful set of microscopic data are the p$k^{1/2}$ values, which characterize the pH value belonging to the 50% degree of protonation. These values are also listed in the last section of Table 3. The data show, in agreement with basic chemical considerations, that a histidine or phenylalanine group (His-BIMA or Phe-His-BIMA) relatively close to the protonation sites somewhat lowers both the amino and imidazole p$k^{1/2}$ values by its electron-withdrawing effect: the amino p$k^{1/2}$ value is decreased to 7.2 in both His- and Phe-containing ligands compared to that of Gly-BIMA (7.8), and the two imidazole p$k^{1/2}$ values are decreased to 2.8 and 5.3 in the His- and Phe-containing ligands compared to the 3.2 and 5.6 values for Gly-BIMA. This effect is relatively weak because of the large distances between the groups.

The deprotonated carboxylic group has the opposite effect, which is assigned to its electron-donating property, causing a rise of the imidazole p$k^{1/2}$ values in BIP (4.4 and 6.9). The raised amino p$k^{1/2}$ value for γ-Glu-BIMA (9.0) can also be assigned to the electron-donating effect of the deprotonated carboxyl group when compared to that of the peptide group. The same effect can be seen when the macroscopic p*K* values for Gly and Gly−Gly [p*K*(amino) = 9.60 and 8.13,[37,38] respectively] are compared.

For the derivatives containing histidine (His-BIMA and Phe-His-BIMA), the deprotonation steps of the imidazole nitrogens and those of the His-imidazole significantly overlap. The effect of the overlapping mainly depends on the position of the His amino acids in the ligands, because the surroundings of the bis-(imidazol-2-yl), and consequently, the p*k* and p$k^{1/2}$ values for the two imidazole groups, are approximately the same for all derivatives. The p$k^{1/2}$ value characterizing the histidine deprotonation is lower for His-BIMA (5.3) than for Phe-His-BIMA (6.0) because of the electron-withdrawing effect of the protonated amino group of His-BIMA. These effects cannot change the deprotonation order for His-BIMA and Phe-His-BIMA (which is imidazole(1)−imidazole(2)−histidine−amino), but they do cause a stronger overlapping in the deprotonation process of His-BIMA, especially for the imidazole(2) and histidine groups.

In the Glu derivatives (α-Glu-BIMA and γ-Glu-BIMA), there is an additional carboxyl group. Its p$k^{1/2}$ value is different for the two studied derivatives. Compared to a carboxyl derivative without any additional groups except for an aliphatic hydrocarbon chain (propionic acid, p*K* = 4.703; *n*-butanoic acid, p*K* = 4.724[39]), the γ-Glu-BIMA ligand has a much lower p*k* value

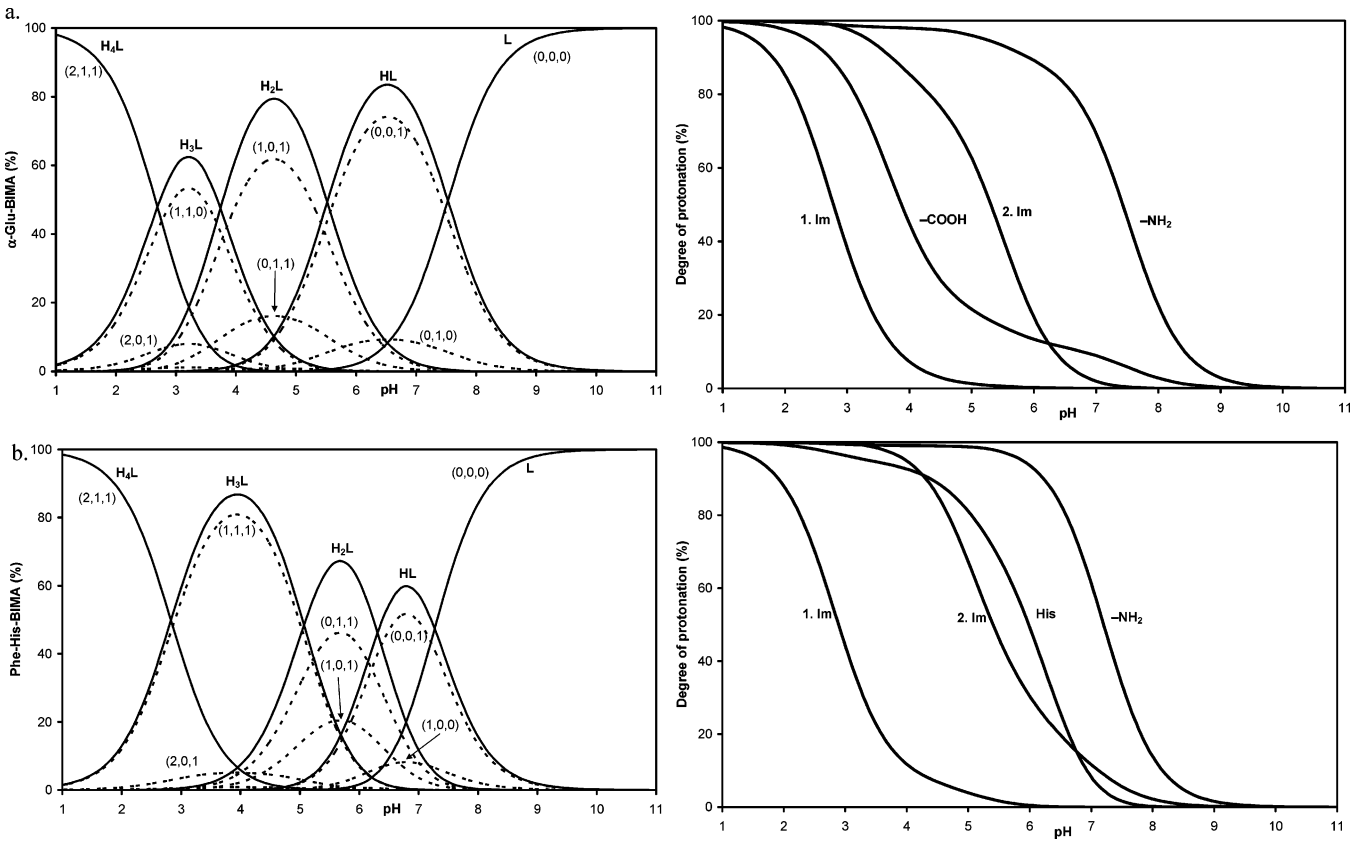

Figure 2. Distribution of the microspecies and the degree of protonation as a function of pH for α-Glu-BIMA (a) and Phe-His-BIMA (b).

owing to the electron-withdrawing effect of the protonated amino group. This effect causes a drastic change in the protonation order, which was also suggested by the macroscopic p*K* values[11] and is proven by the microscopic p*k* values: in γ-Glu-BIMA, the deprotonation sequence is carboxylate−imidazole(1)−imidazole(2)−amino, while in the case of α-Glu-BIMA, it changes to imidazole(1)−carboxylate−imidazole(2)−amino.

The distribution curves of the microspecies and, especially, the figures representing the degree of protonation for a given group as a function of pH [see Figure 2 for α-Glu-BIMA (a) and Phe-His-BIMA (b)] show additional information. In the case of α-Glu-BIMA, the unusually high degree of protonation of the carbonyl group (10% at pH 7) can be attributed to the hydrogen bond between the deprotonated carboxylic and protonated amino groups, resulting in the occurrence of some protons on the carboxyl group at higher pH as well. The strange behavior of the imidazole(2) and histidine deprotonation curves of His-BIMA and Phe-His-BIMA can be explained by the repulsive interactions of the three aromatic rings; the presence of two protonated imidazole rings close to the histidine ring causes, for example, the slight degree of histidine deprotonation at pH 2−5.

To check whether the microequilibrium speciation of these ligands could also be calculated by methods that use protonation-shift coefficients that are transferable between similar structures,[14−24] we calculated the effect of deprotonation at all possible protonation sites on the chemical-shift change of all detected NMR-active nuclei ($\Delta\delta$) using eq 8

$$\Delta\delta = C_{nm}(\delta_{H_nL} - \delta_L) \qquad (8)$$

where δ_{H_nL} and δ_L are the chemical shifts for the fully protonated and deprotonated ligands, respectively. These data show that the $\Delta\delta$ parameters are usually transferable within an acceptable error range, although in a limited number of cases, the difference in these parameters is significant. In other words, the studied ligands are relatively good models of each other. For example, the deprotonation of the two imidazoles causes a 0.524 ppm total shift of the aromatic imidazole NMR signals. This value is 0.502 for Gly-BIMA and γ-Glu-BIMA. These two ligands have the same structure in the bis(imidazolyl) region, and their dominant conformation may also be very similar. The values for BIP and α-Glu-BIMA differ somewhat from the former ones ($\Delta\delta$ = 0.459 and 0.550, respectively). The $\Delta\delta$ parameters for the CH(Im) groups, in the case of imidazole deprotonation, are 0.800, 0.802, 0.846, and 0.805 for BIP, Gly-BIMA, His-BIMA, and Phe-His-BIMA, respectively.

For the amino deprotonation, the $\Delta\delta$ values for the CH (or CH_2) groups two or three bonds away from the deprotonation site show a relatively good agreement: for the two-bond distance, $\Delta\delta$ = 0.555, 0.527, and 0.584 for Gly-BIMA, γ-Glu-BIMA, and Phe-His-BIMA, respectively; for the three-bond distance, $\Delta\delta$ = 0.296, 0.295, and 0.283 for α-Glu-BIMA, γ-Glu-BIMA, and His-BIMA, respectively. The carbonyl deprotonation can be followed in our ligands by the NMR signals two or three bonds away. These values for BIP and α-Glu-BIMA are 0.257 and 0.270, and 0.147 and 0.153, respectively. In summary, although the factors are usually transferable within an acceptable error range for our ligands, this transfer can somewhat increase the error of the calculation. In addition, it is clear that the selection of suitable model ligands requires extreme care. The method presented in this paper avoids this selection step (and the often time-consuming synthesis) and still gives reliable results, as shown by the very similar $\Delta\delta$ factors.

Acknowledgment. The authors acknowledge Prof. Béla Noszál (Eötvös Loránd University of Sciences), Prof. István

Bányai (University of Debrecen), Prof. Imre Sóvágó (University of Debrecen), and László Zékány (University of Debrecen) for their advice. This work was supported by the Hungarian Scientific Research Fund (OTKA T042722, TS040685, and D048488). The helpful suggestions of an anonymous reviewer are also gratefully acknowledged

Supporting Information Available: Normalized chemical shifts of indiviual macrospecies, correlations between macroscopic p*k* values, chemical shifts of observed NMR-active nuclei, distributions of the macrospecies, the degrees of protonation, calculated conditional probablilites, $\Delta\delta$ values, and guidelines for using weights. This information is available free of charge via the Internet at http://pubs.acs.org.

References and Notes

(1) Várnagy, K.; Ösz, K.; Kállay, Cs.; Sóvágó, I. *Prog. Coord. Bioinorg. Chem.* **2003**, *6*, 95.
(2) Sóvágó, I.; Ösz, K.; Várnagy, K. *Bioinorg. Chem. Appl.* **2003**, *1*, 123.
(3) Ösz, K.; Várnagy, K.; Süli-Vargha, H.; Csámpay, A.; Sanna, D.; Micera, G.; Sóvágó, I. *J. Inorg. Biochem.* **2004**, *98*, 24.
(4) Ösz, K.; Várnagy, K.; Süli-Vargha, H.; Sanna, D.; Micera, G.; Sóvágó, I. *J. Chem. Soc., Dalton Trans.* **2003**, 2009.
(5) Ösz, K.; Várnagy, K.; Süli-Vargha, H.; Sanna, D.; Micera, G.; Sóvágó, I. *Inorg. Chim. Acta* **2002**, *339*, 373.
(6) Sóvágó, I.; Várnagy, K.; Ösz, K. *Comments Inorg. Chem.* **2002**, *23*, 149.
(7) Ösz, K.; Várnagy, K.; Sóvágó, I.; Lennert, L.; Süli-Vargha, H.; Sanna, D.; Micera, G. *New J. Chem.* **2001**, *25*, 700.
(8) Várnagy, K.; Sóvágó, I.; Süli-Vargha, H.; Sanna, D.; Micera, G. *J. Inorg. Biochem.* **2000**, *81*, 35.
(9) Várnagy, K.; Sóvágó, I.; Ágoston, K.; Likó, Zs.; Süli-Vargha, H.; Sanna, D.; Micera, G. *J. Chem. Soc., Dalton Trans.* **1994**, 2939.
(10) Várnagy, K.; Sóvágó, I.; Goll, W.; Süli-Vargha, H.; Micera, G.; Sannad, D. *Inorg. Chim. Acta* **1998**, *283*, 233.
(11) Kállay, Cs.; Cattari, M.; Sanna, D.; Várnagy, K.; Süli-Vargha, H.; Csámpai, A.; Sóvágó, I.; Micera, G. *New J. Chem.* **2004**, *28*, 727.
(12) Kiss, T.; Sóvágó, I.; Martin, R. B. *Polyhedron* **1991**, *10*, 1401.
(13) Kurzak, B.; Kozlowski, H.; Farkas, E. *Coord. Chem. Rev.* **1992**, *114*, 2215.
(14) Rabenstein, D. L.; Sayer, T. L. *Anal. Chem.* **1976**, *48*, 1141.
(15) Juy, M.; Lam-Thanh, H.; Lintner, K.; Fermandjian, S. *Int. J. Pept. Protein Res.* **1983**, *22*, 437.
(16) Xu, G.; Evans, J. S. *Biopolymers* **1999**, *49*, 303.
(17) Cabezas, E.; Satterthwait, A. C. *J. Am. Chem. Soc.* **1999**, *121*, 3862.
(18) Opitz, N.; Merten, E.; Acker, H. *Pflugers Arch.* **1994**, *427*, 332.
(19) Gilbert, D.; Goodford, P. J.; Norrington, F. E.; Weatherley, B. C.; Williams, S. G. *Br. J. Pharmacol.* **1975**, *55*, 117.
(20) Beilharz, G. R.; Smith, J. A.; Austen, K. F.; Wright, P. E. *Int. J. Pept. Protein Res.* **1985**, *25*, 337.
(21) Noszál, B.; Rabenstein, D. L. *J. Phys. Chem.* **1991**, *95*, 4761.
(22) Noszál, B.; Szakács, Z. *J. Phys. Chem. B* **2003**, *107*, 5074.
(23) Santos, M. A.; Esteves, M. A.; Vaz, M. C.; da Silva, J. J. R. F.; Noszál, B.; Farkas, E. *J. Chem. Soc., Perkin Trans. 2* **1997**, 1977.
(24) Noszál, B. *J. Phys. Chem.* **1986**, *90*, 4104.
(25) Drey, D. N. C.; Fruton, J. S. *Biochemistry* **1965**, *4*, 1.
(26) Irving, H.; Miles, G.; Petit, L. D. *Anal. Chim. Acta* **1967**, *38*, 475.
(27) Zékány, L.; Nagypál, I. In *Computational Methods for the Determination of Stability Constants*; Leggett, D., Ed.; Plenum Press: New York, 1985; pp 291−299.
(28) Munowitz, M.; Bachovchin, W. W.; Herzfeld, J.; Dobson, C. M.; Griffin, R. G. *J. Am. Chem. Soc.* **1982**, *104*, 1192.
(29) Purlee, E. L. *J. Am. Chem. Soc.* **1959**, *81*, 263.
(30) Mikkelsen, K.; Nielsen, S. O. *J. Phys. Chem.* **1960**, *64*, 632.
(31) Glasoe, P. K.; Long, F. A. *J. Phys. Chem.* **1960**, *64*, 188.
(32) Krezel, A.; Bal, W. *J. Inorg. Biochem.* **2004**, *98*, 161.
(33) Dailey, B. P.; Shoolery, J. N. *J. Am. Chem. Soc.* **1955**, *77*, 3977.
(34) Grunwald, E.; Loewenstein, A.; Meiboom, S. *J. Chem. Phys.* **1957**, *27*, 641.
(35) Ullmann, G. M. *J. Phys. Chem. B* **2003**, *107*, 1263.
(36) Szakács, Z.; Noszál, B. *J. Math. Chem.* **1999**, *26*, 139.
(37) Kim, M. K.; Martell, A. E. *Biochemistry* **1964**, *3*, 1169.
(38) Kiss, T.; Sóvágó, I.; Gergely, A. *Pure Appl. Chem.* **1991**, *63*, 597.
(39) Cannon, R.; Kibrick, A. *J. Am. Chem. Soc.* **1938**, *60*, 2314.